Available online at www.sciencedirect.com
ScienceDirect
Journal of the European Ceramic Society 29 (2009) 1513–1519
www.elsevier.com/locate/jeurceramsoc

Optimized vacuum/pressure sol impregnation processing of wood for the synthesis of porous, biomorphic SiC ceramics

J. Locs [a,*], L. Berzina-Cimdina [a], A. Zhurinsh [b], D. Loca [a]

[a] *Riga Technical University, Riga Biomaterials Innovation and Development Center, Pulka Street 3/3, LV-1007 Riga, Latvia*
[b] *Latvian State Institute of Wood Chemistry, Dzerbenes Street 27, LV-1006 Riga, Latvia*

Received 10 September 2008; accepted 20 September 2008
Available online 28 October 2008

Abstract

Pine (*Pinus silvestris*) wood with shaped sample dimensions of 20 mm × 20 mm × 5 mm (axial) was selected as the raw material. Samples were dried and, for a half of the samples, resin extraction from the sample was applied. SiO_2 sol was prepared, and samples were impregnated under different vacuum/pressure conditions. Relative impregnation efficiency was calculated for impregnated samples and varied from 95 up to 105% of the theoretical value for different samples and impregnation conditions. Impregnation and drying procedures were repeated up to three times to increase the SiO_2 amount introduced in the sample. Impregnated samples were pyrolyzed at 500 °C under oxygen free atmosphere with the subsequent high temperature treatment at 1600 °C in an Ar atmosphere. Biomorphic SiC ceramics and its precursors were investigated using X-ray diffraction (XRD), Fourier transform infrared spectroscopy (FT-IR) and scanning electron microscopy (SEM). An experimental result shows that the optimized vacuum/pressure impregnation technique is highly effective for the introduction of SiO_2 in the wood.

Keywords: Sol–gel process; Porosity; SiC; Wood

1. Introduction

Nowadays, nature is progressively becoming a model for innovation in structural design. Recently, a new class of structural materials, biomorphic ceramics, has attracted a lot of attention. These materials are prepared by the biotemplating technique, where natural grown structures are used as bulk templates for fast high-temperature conversion into ceramics. Bioorganic substances like wood are characterized by a strongly anisotropic structure, where the basic units are elongated channels, assembled parallel to the growth direction. The advantage of wood as a structural material is the durability of the structure combined with a low bulk density. The introduction of Si in the wood offers possibilities of obtaining porous SiC ceramics during high temperature treatment in an inert atmosphere.

Up to know, there are several technologies developed for obtaining porous SiC ceramic materials from wood precursors, some of them being reactive Si vapor infiltration,[1–6] infiltration with Si containing vapors from decomposed metal organic precursors,[7] and reactive infiltration with Si-containing melts.[8–13] Impregnation with SiO_2 nanoparticles containing sol,[14–17] with $Na_2O{\cdot}nSiO_2$,[18] with Si-containing polymer,[19] with metal organic precursors[20–24] and with sol–gel derived SiO_2 sol[25] was performed *via* the following carbothermal reactions. Comparing the previously mentioned methods, the sol–gel impregnation method with the following carbothermal reaction has some advantages such as low cost, easy procedure and the ability to retain the structure and morphology of the starting carbonaceous precursor material. As a result of the reactions, single-phase SiC ceramics with a relatively high porosity is commonly obtained.[25]

For obtaining of porous SiC ceramics, the optimized vacuum/pressure SiO_2 sol impregnation technique was developed and described in the present paper. In the previously published papers, impregnation has been repeated up to 5 times with each impregnation process time up to 9 h to achieve the optimal C to SiO_2 molar ratio ≈3 in the sample;[26] after four impregnation procedures, only 45% of the $Si(OH)_4$-gel weight gain necessary for the complete reaction has been achieved.[27] Unlike described in previous studies[15] that sol gradients and uneven infiltration causes 50% difference between calculated and measured infiltration results in the wood state, IE up to 95% for non-extracted and

* Corresponding author. Tel.: +371 67089605; fax: +371 67089619.
E-mail address: janis.locs@rtu.lv (J. Locs).

0955-2219/$ – see front matter © 2008 Elsevier Ltd. All rights reserved.
doi:10.1016/j.jeurceramsoc.2008.09.013

105% for extracted pine wood samples have been achieved. The use of the optimized process allows decreasing the number of impregnation cycles to three and shortening the total one impregnation procedure time to about 40 min. For the impregnation procedure, pine tree (*Pinus silvestris*) samples were prepared and, for a half of them, resin extraction was performed. After each impregnation, gelling and drying of SiO_2 gel were carried out, forming the SiO_2 gel/wood composite. The impregnation procedure was repeated several times to increase the SiO_2 content in the sample. Pyrolysis of the obtained samples was done to convert the SiO_2 gel/wood composite into a SiO_2/C_B (biocarbon) composite. The following high temperature treatment in an Ar atmosphere leads to the carbothermal SiO_2 and C_B reaction, forming porous SiC ceramics with a tubular, pine wood specific structure. The microstructure, crystalline phase composition and chemical functional groups of biomorphic SiC ceramics and its precursors were investigated using X-ray diffraction (XRD), Fourier transform infrared spectroscopy (FT-IR) and scanning electron microscopy (SEM).

2. Experimental procedure

2.1. Material preparation

Pine wood was shaped in dimensions of 20 mm × 20 mm × 5 mm (axial) and dried at 105 °C for 24 h. To increase the pore volume and the corresponding possible amount of the impregnated Si precursor per cycle, resin extraction was applied for a half of the samples. Extraction was performed in a Soxlet extraction apparatus for 24 h; toluene/ethanol solution in the volume ratio 2:1 was used as the solvent. SiO_2 sol was prepared using TEOS – tetraethyl orthosilicate (Aldrich, Ref.: 131903), distilled water, hydrochloric acid and ethanol at a suitable molar ratio to obtain the concentration of SiO_2 sol equal to ≈15% by weight.

Wood samples were placed in a self-made impregnation vessel, evacuated for 5 min up to a 52 kPa vacuum, then showered with SiO_2 sol and delayed for 5 min before the pressure increasing in the vessel up to the atmospheric pressure. Then the samples and SiO_2 sol were moved to a custom-made hydraulic isostatic press with the following pressure increase up to 30, 60, 125 MPa with a 5 min hold time. After high-pressure treatment, the samples were drained and weighed to determine the SiO_2 sol uptake and placed in a drying oven applying an increasing temperature up to 105 °C with the hold time 24 h at the maximum temperature. After each impregnation cycle, which included impregnation and drying, mass increase of the sample was measured. Impregnation cycles were repeated three times to increase the SiO_2 content in the sample. Pyrolysis of the samples was performed in an oxygen-free atmosphere at 500 °C with the rate 120 °C/h to form a SiO_2/C_B composite. Further sample processing was performed in a modified high-temperature furnace in an Ar atmosphere for 1600 °C with the rate 300 °C/h. The temperature in the furnace was raised up to the desired temperature and hold for 4 h to conduct the carbothermal reaction between SiO_2 and C_B, resulting in the formation of β-SiC. Fig. 1 represents a flow diagram of the whole process.

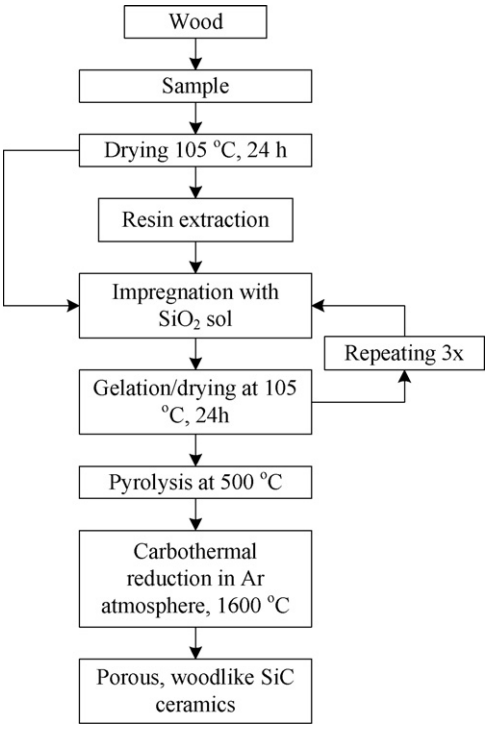

Fig. 1. Flow diagram of manufacturing biomorphic SiC ceramics from pine wood.

2.2. Characterization

The pyrolytic behavior of pine tree wood, SiO_2 gel and the SiO_2 gel/wood composite was characterized using thermogravimetric analysis (TGA) and differential thermal analysis (DTA) in a N_2 atmosphere with the flow rate 20 ml/min (TGA) and 100 ml/min (DTA), with the heating rate 5 °C/min from room temperature to 1000 °C. TGA and DTA were performed on a TGA/SDTA 841 (Mettler Toledo) thermal analyzer.

A Fourier transformation infrared spectrometer (Varian Scimitar 800) in the wave number range 4000–400 cm^{-1} was used for sample investigations in the transmission mode in a dry air atmosphere using the KBr pellet technology.

For crystalline phase identification, X-ray diffraction was measured on a powder X-ray diffractometer (PANalytical X'Pert Pro), using Cu radiation produced at 40 kV and 30 mA, step size of 0.017° (2θ), and a hold time of 20 s.

The morphological properties of the samples were investigated using a scanning electron microscope (Tescan Mira/LMU) at 20 kV acceleration voltage and 6–10 mm working distance. For the observation sample fracture surface was used. 15 nm gold film was sputtered on the samples before the observation.

3. Results and discussion

3.1. Resin extraction, impregnation efficiency

During resin extraction, resins were removed from the resin canals. The average weight loss of the samples was 2 mass%. As an indicator of this is the Impregnation Efficiency (IE, %), respectively, the volume share in percent from the total theoret-

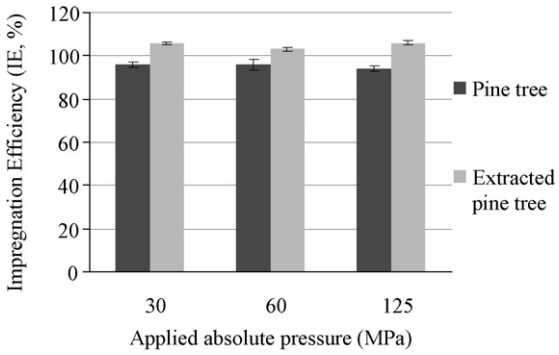

Fig. 2. Relationship between IE and the applied absolute pressure for pine wood and extracted pine wood samples.

ical pore volume filled with SiO_2 sol right after impregnation (see Fig. 2), calculated for the first impregnation cycle using Eq. (1).

$$\mathrm{IE} = \frac{\rho_s \cdot \rho_w \cdot m_{sol}}{\rho_{sol} \cdot m_s(\rho_w - \rho_s)} \cdot 100\% \quad (1)$$

where ρ_s: sample geometrical density (g/cm^3); ρ_w: specific gravity of a lignified cellulose cell wall, 1.53 g/cm^3; m_{sol}: weight of the impregnated SiO_2 sol in the sample (g); ρ_{sol}: density of SiO_2 sol (g/cm^3); m_s: weight of the sample before impregnation (g).

The sample geometrical density (ρ_s, g/cm^3) before impregnation was found to be 0.523 ± 0.011 g/cm^3 for extracted and 0.535 ± 0.014 g/cm^3 for non-extracted samples. The specific gravity of a lignified cellulose cell wall, 1.53 g/cm^3, is practically constant for all timbers.[28] The density of the prepared SiO_2 sol was measured using the gravimetric method and was 0.872 ± 0.002 g/cm^3. The comparison of IE for pine wood and extracted pine wood applying different pressures is shown in Fig. 2. For pine wood, IE varies around 95%, while, for extracted pine wood IE reaches 105%. So, the high IE results for the extracted pine wood can be explained by filling of the emptied and opened resin canals and a better SiO_2 sol/cell wall wetting ability. The extracted pine wood IE was calculated against the theoretical free volume of the non-extracted pine wood.

3.2. SiO_2 content in the samples, pyrolysis and TGA/SDTA analysis

For complete conversion of the carbon present in wood to SiC during carbothermal reactions, a notable amount of SiO_2 should be introduced in the sample. The total SiO_2 to C_B mass ratio should be around 1.67. As there is a mass decrease for the SiO_2 gel and wood during pyrolysis, mass yield for both of them was determined. It was established that the char yield of wood dried at 105 °C after pyrolysis at 500 °C (C_B) was 23.5 wt.%, and that of the SiO_2 gel dried at 105 °C after the treatment at 1000 °C (Y_{gel}) was 94 wt.%. Considering the above-mentioned, the dried gel mass m_g (g) to m_s ratio (coefficient K) was calculated using Eq. (2). In our case, the theoretical value of K was equal to 0.41.

$$K = \frac{m_g}{m_s} = \frac{1.67 \cdot C_B}{Y_{gel}} \quad (2)$$

Table 1
Coefficient K values after three impregnation cycles with SiO_2 sol.

	Applied absolute pressure, MPa		
	30	60	125
Extracted pine wood	0.63 ± 0.04	0.58 ± 0.01	0.62 ± 0.03
Pine wood	0.61 ± 0.04	0.54 ± 0.02	0.61 ± 0.03

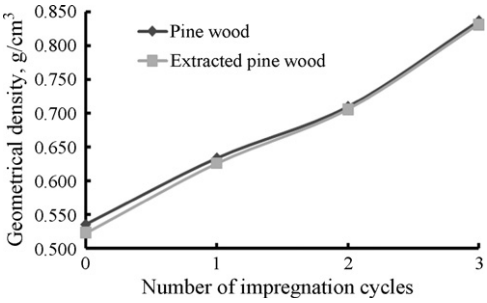

Fig. 3. Relationship between the geometrical density of the SiO_2 gel/pine wood composite and the number of impregnation cycles.

Table 1 shows calculated coefficient K values for the experimental samples. There is no significant difference between the extracted and non-extracted samples as well as between the applied pressures. Lower K values at the applied pressure 60 MPa in both cases cannot be explained before extra investigations. The overall results show that, in three cycles, it is possible to introduce the necessary SiO_2 amount in the wood for SiC synthesis.

The geometrical density of the samples as well as their mass increases after each impregnation cycle. Fig. 3 shows that the density of pine wood is 0.52 g/cm^3 for extracted and 0.53 g/cm^3 for non-extracted samples and rapidly increases as the number of impregnation cycles increases. After three impregnation cycles, the geometrical density of both extracted and non-extracted samples reached 0.83 g/cm^3. During pyrolysis, not only the samples' weight loss occurs, but also the geometrical dimensions decrease as described in Table 2. The impregnated sample's dimension changes in tangential, radial and axial directions are 6, 7 and 17% less than for the reference pine wood samples. It was observed that such SiO_2 gel effect on the sample dimension changes during pyrolysis does not lead to the formation of cracks in the cell walls. It can be concluded that no reasonable internal stress appears in C_B cell walls. After pyrolysis, geometrical density for extracted and non-extracted samples was 0.83 g/cm^3.

Mass changes during pyrolysis were investigated using TGA and are shown in Fig. 4. Generally, wood starts to degrade ther-

Table 2
Dimension changes for the three times impregnated sample after pyrolysis at 500 °C.

Samples	Change of dimensions (%)		
	Tangential	Radial	Axial
Extracted, impregnated pine wood	25.5 ± 2.1	18.9 ± 1.7	8.2 ± 1.6
Impregnated pine wood	25.6 ± 1.4	19.4 ± 0.9	8.5 ± 0.7
Pine wood	31.2 ± 1.3	26.6 ± 1.3	15.2 ± 1.2

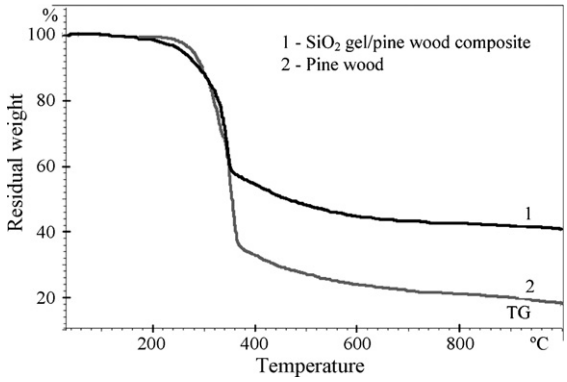

Fig. 4. TG curves of the SiO_2 gel/pine wood composite and the reference pine wood sample.

mally at about 250 °C. The SiO_2 gel/wood composite begins to degrade earlier at 220 °C owing to the residual ethyl groups in the SiO_2 gel. Between about 300–375 °C, the majority of wood-containing polymers have degraded. At about 400 °C, the pyrolysis process is finished and, during further rising of temperature, mainly the oxygen and hydrogen amount in C_B decreases. At 500 °C, mainly all mass changes have occurred, and only a small decrease in mass continues with increasing temperature.

DTA curves of the SiO_2 gel/pine wood composite and the reference pine wood sample are shown in Fig. 5. There are no considerable differences between both curves, which indicate that the SiO_2 gel does not lead to a significant influence on thermal processes of pyrolysis.

3.3. FT-IR analysis

Fig. 6 shows the FT-IR spectra of pine wood, SiO_2 gel (dried at 105 °C) and three times impregnated SiO_2 gel/pine wood composite. In the spectrum (Fig. 6a and c) of the pine wood and SiO_2 gel/pine wood composite, the absorption bands at 3380 and 1113 cm^{-1} are attributed to the O–H stretch vibration and the association band in cellulose and hemicellulose. Another characteristic absorption band of wood is located at 2928 cm^{-1} and is ascribed to the C–H stretch vibration. The C–O stretch vibrations absorption band in cellulose and hemicelluloses is at 1055 cm^{-1}, and this is the highest intensity band.[29] In the spectrum (Fig. 6b) of the SiO_2 gel, the absorption bands at 1090, 800 and 460 cm^{-1} are ascribed to the asymmetric and symmetric stretching vibrations of Si–O–Si and Si–OH bonds.[25] In the SiO_2 gel/pine wood composite FT-IR absorption spectrum (Fig. 6c), peaks characteristic for both pine wood and SiO_2 gel absorption spectra appear, suggesting that no chemical reaction between the SiO_2 gel and wood occurs during the impregnation cycle.

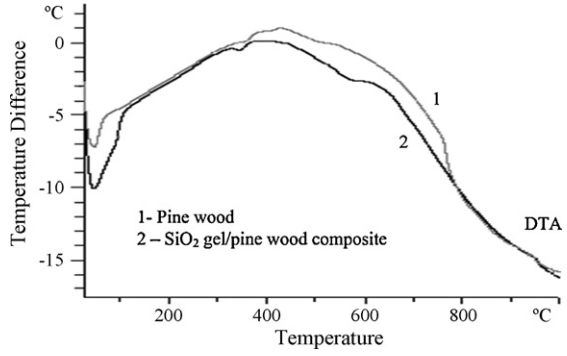

Fig. 5. DTA curves of the SiO_2 gel/pine wood composite and the reference pine wood sample.

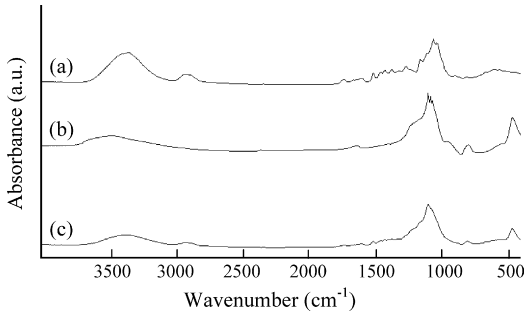

Fig. 6. FT-IR spectra of pine wood (a), SiO_2 gel (b) and SiO_2 gel/pine wood composite (c).

Fig. 7 shows the FT-IR spectra of the SiO_2/C_B composite after pyrolysis (Fig. 7a) and the SiC ceramics obtained at 1600 °C in an inert atmosphere for 4 h (Fig. 7b). In the SiO_2/C_B composite spectrum, asymmetric and symmetric stretching vibrations of Si–O–Si bonds at 1090, 800 and 460 cm^{-1} and C_B characteristic C=C bond vibrations at 1600 cm^{-1} can be observed. In the FT-IR spectrum of the products obtained at 1600 °C, the peaks assigned to Si–O and C=C bonds become negligible, and nearly only the peaks ascribed to the Si–C fundamental stretching vibration at 825 cm^{-1} exist, suggesting that carbothermal reduction is nearly completed.[25]

3.4. XRD analysis

The XRD patterns of the SiO_2 gel dried at 105 °C, pine wood and the SiO_2 gel/pine wood composite dried at 105 °C are shown in Fig. 8. It can be seen that two broad peaks centered at $2\theta = 24°$ and 44° in Fig. 8a suggest that the SiO_2 gel is in an amorphous state. In Fig. 8b, the characteristic peak of cellulose crystals centered at $2\theta = 22°$ can be found.[30] Characteristic peaks of both SiO_2 gel and pine wood can be found in Fig. 8c. The cellulose characteristic peak centered at $2\theta = 22°$ overlap the SiO_2 gel relevant peak centered at $2\theta = 24°$, resulting in a peak centered

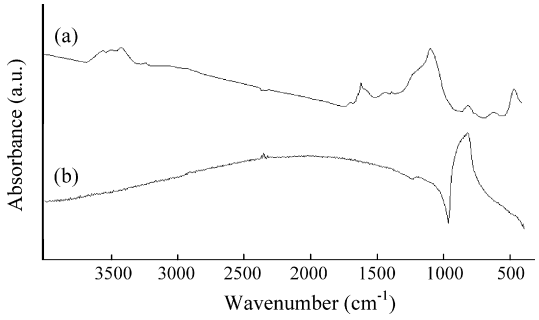

Fig. 7. FT-IR spectra of the SiO_2/C_B composite after pyrolysis (a) and the SiC ceramics obtained at 1600 °C (b).

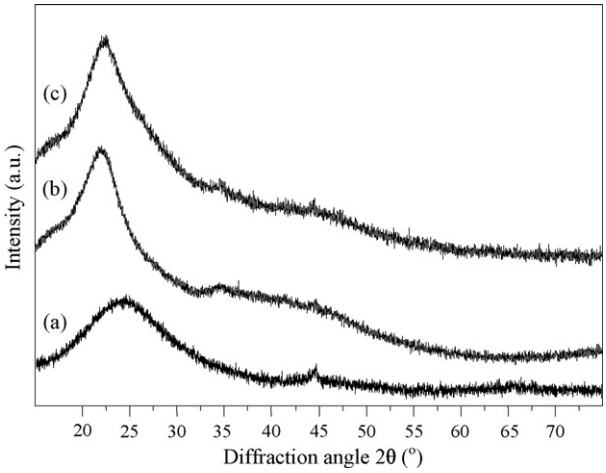

Fig. 8. XRD patterns of the SiO_2 gel (a), pine wood (b) and SiO_2 gel/pine wood composite (c).

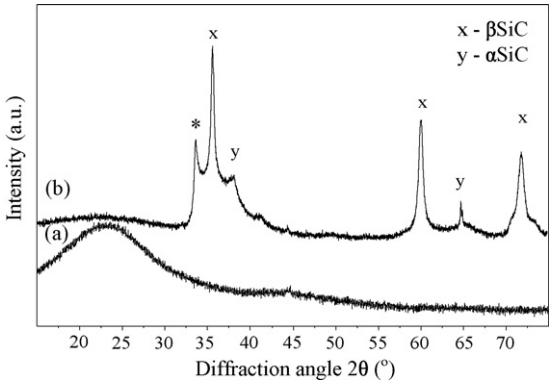

Fig. 9. XRD patterns of the SiO_2/C_B composite (a) and the obtained porous biomorphic SiC ceramics (b).

at $2\theta = 22.5°$. The peak characteristic for SiO_2 gel at $2\theta = 44°$ shown in Fig. 8c has a lower intensity than that shown in Fig. 8a.

The XRD patterns of the SiO_2/C_B composite obtained at 500 °C and the porous biomorphic SiC ceramics obtained at 1600 °C are shown in Fig. 9. It can be suggested that the broad peak centered at $2\theta = 24°$ is formed by overlapping the C_B characteristic peak[22] and the amorphous SiO_2 characteristic peak, both located at around $2\theta = 24°$. In the XRD pattern of the products obtained at 1600 °C, peaks of major phase cubic type β-SiC appear. Some amount of hexagonal α-SiC was found characterized by additional peaks around $2\theta = 38°$ and 65°. An additional diffraction peak (* marked) was detected at $2\theta = 33.68°$, which is characteristic for stacking faults on the [1 1 1] planes in cubic SiC.[31] Diffraction peaks for crystalline SiO_2 (crystobalite) are never observed, which indicates that nearly the whole amount of silica has been consumed during the carbothermal reduction. As the K values for obtained samples was larger than theoretical ones but XRD do not confirm residue of SiO_2 in the sample, it is supposed that the rest SiO_2 left the sample during carbothermal

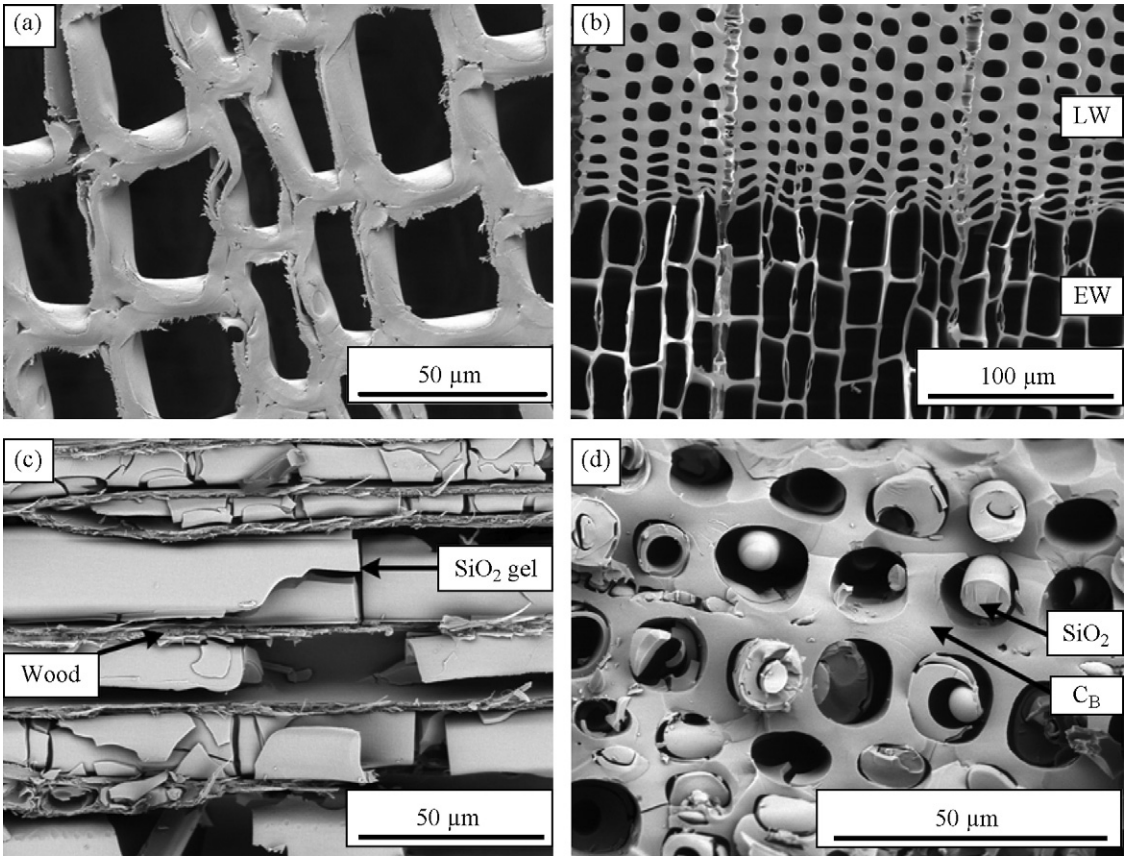

Fig. 10. SEM micrographs of pine wood (a), pine wood C_B template (LW, late wood; EW, early wood) (b), three times impregnated SiO_2 gel/pine wood composite (c) and SiO_2/C_B composite (d).

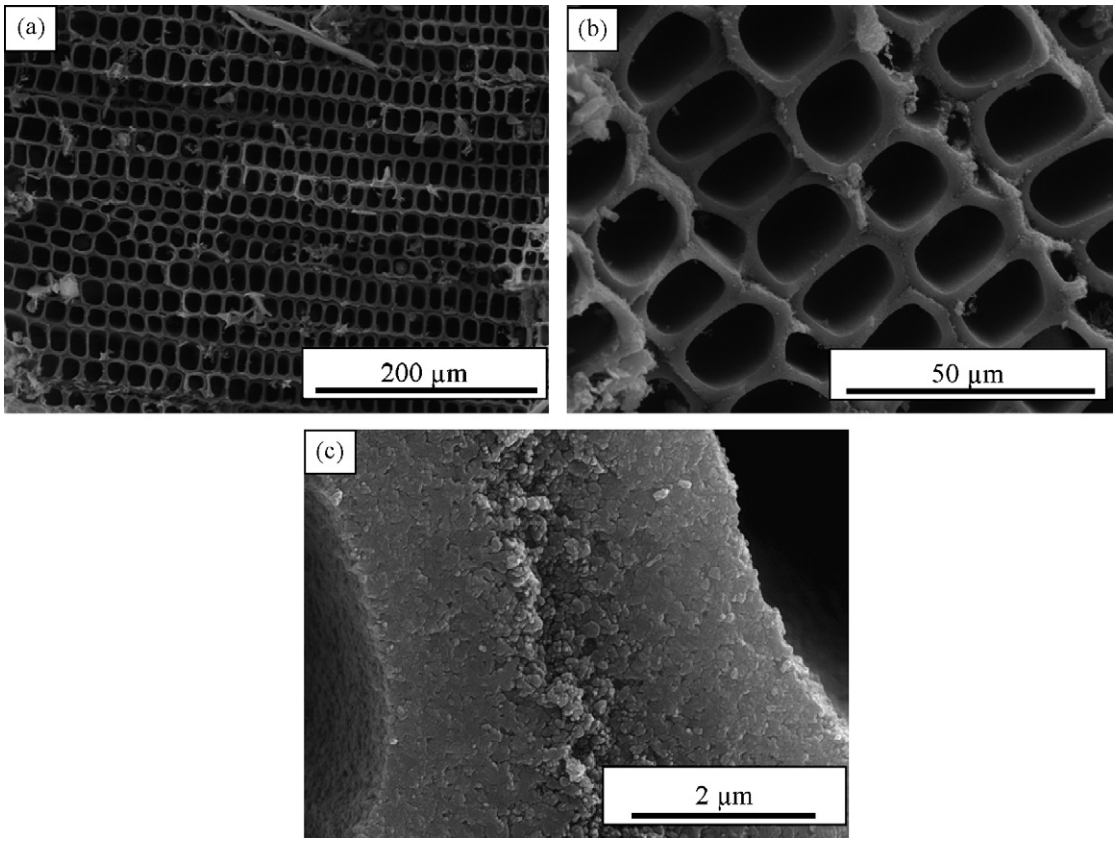

Fig. 11. SEM micrographs of porous SiC ceramics.

reduction and condensed on the crucible walls, where glass type coating after several experiments was observed. The shape of the peaks indicates that the obtained products are fine-crystalline ceramics.

3.5. SEM analysis

SEM micrographs of pine wood, pine wood C_B charcoal, the SiO_2 gel/pine wood composite and the SiO_2/C_B composite are shown in Fig. 10. The transverse section of pine wood is shown in Fig. 10a. In pine wood tracheids with the mean diameter 20–40 μm and 5–10 μm cell wall thickness forms a tubular structure. The tracheids can have a round or rectangular shape. Fig. 10b shows a transverse section of pyrolyzed pine wood. As can be seen, late wood is formed of round shape tracheids with a thinner cell wall than the early wood tracheids of rectangular shape.

After the pine wood is impregnated with SiO_2 sol, subsequent gelling and drying occur, and a SiO_2 gel/wood composite is formed (see the radial section in Fig. 10c). It can be seen that the gel fills almost all tracheids. The cracks in the gel may occur during the drying procedure of the gel or sample preparation. After pyrolysis, a SiO_2/C_B composite is formed (Fig. 10d). As there were several impregnation procedures performed, all three shells of impregnated SiO_2 can be seen in some pores.

The mechanism of conversion of the SiO_2/C_B composite into SiC ceramics is widely described by Qian et al.[26]. In Fig. 11, SEM micrographs of porous SiC ceramics, obtained at 1600 °C for 4 h, are shown. As can be seen, the obtained ceramic materials retain the tubular pore structure of pine wood. The geometrical density of the obtained samples was measured, to be equal to 0.35 g/cm^3. As the density of β-SiC is 3.21 g/cm^3, the overall porosity of the samples was calculated to be 89%.

It has been found from SEM micrographs that the pore walls are formed of SiC crystals with the average size 100 nm (Fig. 11c).

4. Conclusions

Optimized process, described in this paper demonstrates the technology for manufacture porous SiC ceramics, using pine wood and TEOS as raw materials. The optimized process allows easily in short time procedures to introduce the necessary amount of the SiO_2 for full conversion of the carbon present in pine wood into SiC.

Simplified Impregnation Efficiency (IE, %) calculation is introduced as an impregnation indicator. IE up to 95% for non-extracted and 105% for extracted pine wood samples can be achieved.

There is no significant difference in the SiO_2 uptake between the pressures applied.

It is concluded from FTIR spectra that no chemical reaction between SiO_2 gel/wood and SiO_2/C_B in composites occurs.

The effect of SiO_2 gel on the sample dimension changes during pyrolysis does not lead to the formation of cracks in the cell walls.

Acknowledgements

This work has been partly supported by the European Social Fund within the National Program "Support for carrying out doctoral study programs and post-doctoral researches", project "Support for the development of doctoral studies at the Riga Technical University".

References

1. Esposito, L., Pinacastelli, A., Melandri, C. and Fabbriche, D. D., Microstructure and compressive strength of sorous SiC serived from wood. *Key Eng. Mater.*, 2004, **246–268**, 2195–2198.
2. Guanjun, Q., Rong, M., Ning, C., Chunguang, Z. and Zhihao, J., Microctructure transmissibility in preparing SiC ceramics from natural wood. *J. Mat. Process. Tech.*, 2002, **120**, 107–110.
3. Vogli, E., Mukerji, J. and Hoffmann, C., Conversion of oak to cellular silicon carbide ceramic by gas-phase reaction with silicon monoxide. *J. Am. Ceram. Soc.*, 2001, **84**, 1236–1240.
4. Vogli, E., Sieber, H. and Greil, P., Biomorphic SiC-ceramic preparated by Si-vapor phase infiltration of wood. *J. Eur. Ceram. Soc.*, 2002, **22**, 2663–2668.
5. Esposito, L., Piancastelli, A., Melandri, C. and Fabbriche, D. D., Microstructure and compressive strenght of porous SiC derived from wood. *Key Eng. Mater.*, 2004, **264–268**, 2195–2198.
6. Qian, J.-M., Wang, J.-P. and Jin, Z.-H., Preparation and properties of porous microcellurar SiC ceramics by reactive infiltration of Si vapor into carbonized brasswood. *Mater. Chem. Phys.*, 2003, **82**, 648–653.
7. Greil, P., Vogli, E., Fey, T. *et al.*, Effect of microstructure on the fracture behavoir of biomorphous silicon carbide ceramics. *J. Eur. Ceram. Soc.*, 2002, **22**, 2697–2707.
8. Singh, M. and Salem, J. A., Mechanical properties and microstructure of biomorphic silicon carbide ceramics fabricated from wood precursors. *J. Eur. Ceram. Soc.*, 2002, **22**, 2709–2717.
9. Munoz, A., Fernandez, J. M. and Singh, M., High temperature compressive mechanical behavior of joined biomorphic silicon carbide ceramics. *J. Eur. Ceram. Soc.*, 2002, **22**, 2727–2733.
10. Varela-Feria, F. M., Martinez-Fernandez, J., Arellano-Lopez, A. R. and Singh, M., Low density biomorphic silicon carbide: microstructure and mechanical properties. *J. Eur. Ceram. Soc.*, 2002, **22**, 2719–2725.
11. Esposito, L., Sciti, D., Pinacastelli, A. and Bellosi, A., Microstructure and properties of porous β-SiC templated from soft woods. *J. Eur. Ceram. Soc.*, 2004, **24**, 533–540.
12. Zollfrank, C. and Sieber, H., Microstructure and phase morphology of wood derived biomorphous SiSiC-ceramics. *J. Eur. Ceram. Soc.*, 2004, **24**, 495–506.
13. Hofenauer, A., Treusch, O., Troger, F. *et al.*, Dense reaction infiltrated silicon/silicon carbide ceramics derived from wood based composites. *Adv. Eng. Mat.*, 2003, **5**(11), 794–799.
14. Klinger, R., Sell, J., Zimmermann, T. *et al.*, Wood-delivered porous ceramics via infiltration of SiO_2-sol and carbothermal reduction. *Holzforschung*, 2003, **57**, 440–446.
15. Herzog, A., Klingner, R., Vogt, U. and Graule, T., Wood-derived porous SiC ceramics by sol infiltration and carbothermal reduction. *J. Am. Ceram. Soc.*, 2004, **87**, 784–793.
16. Vogt, U., Herzog, A., Graule, T. *et al.*, Porous ceramics derived from wood. *Key Eng. Mater.*, 2002, **206–213**, 1941–1944.
17. Furuno, T. and Fujisawa, M., Carbonisation of wood-silica composites and formation of silicon carbide in the cell wall. *Wood Fiber Sci.*, 2004, **36**(2), 269–277.
18. Vyshnyakova, K., Yushin, G., Pereselentseva, L. and Gogotsi, Y., Formation of porous SiC ceramics by pyrolysis of wood impregnation with silica. *J. Apll. Ceram. Technol.*, 2006, **3**(6), 485–490.
19. Zollfrank, C., Kladny, R., Sieber, H. and Greil, P., Biomorphous SiOC/C-ceramic composites from chemically modified wood templates. *J. Eur. Ceram. Soc.*, 2004, **24**, 479–487.
20. Shin, Y., Wang, L., Liu, J. and Exarhos, G., pH-Controlled synthesis of hierarchially ordered ceramics with wood cellular structures by surfactant-directed sol-gel procedure. *J. Ind. Eng. Chem.*, 2003, **9**, 76–82.
21. Persson, P. V., Hafren, J. and Fogden, A., Silica nanocasts of wood fibers: A study of cell-wall accessibility and structure. *Biomacromolecules*, 2004, **5**, 1097–1101.
22. De Castro, L. Sol–gel method of making silicon carbide and of protecting a substrate. Pat. US5256448 (11.11.1991).
23. Ota, T., Takahashi, M., Hibi, T., Ozawa, M., Suzuki, S. and Hikichi, Y., Biomimetic process for producting SiC "Wood". *J. Am. Ceram. Soc.*, 1995, **78**, 3409–3411.
24. Castro, V., Fujisawa, M., Hata, T. *et al.*, Silicon carbide nanorods and ceramics from wood. *Key Eng. Mater.*, 2004, **264–268**, 2267–2270.
25. Qian, J.-M. and Jin, Z.-H., Preparation and characterization of porous, biomorphic SiC ceramic with hybrid pore structure. *J. Eur. Ceram. Soc.*, 2006, **24**, 1311–1316.
26. Qian, J.-M., Wang, J.-P., Qiao, G.-J. and Jin, Z.-H., Preparation of porous SiC ceramic with a woodlike microstructure by sol-gel and carbothermal reduction processing. *J. Eur. Ceram. Soc.*, 2004, **24**, 3251–3259.
27. Rambo, C. R., Cao, J., Rusina, O. and Sieber, H., Manufacturing of biomorphic (Si, Ti, Zr)-carbide ceramics by sol-gel processing. *Carbon*, 2005, **43**, 1174–1183.
28. Usta, I., Comparative Study of Wood Density by Specific Amount of Void Volume (Porosity). *Turk. J. Agric. For.*, 2003, **27**, 1–6.
29. Rowell, R. M., *Handbook of wood chemistry and wood composites*. Taylor & Francis, Boca Raton, Florida, 2005, p. 196.
30. Borysaik, S. and Doczekalska, B., X-ray diffraction study of pine wood treated with NaOH. *Fibers Textilies Easten Eur.*, 2005, **13**(5), 87–89.
31. Shin, Y., Wang, C., Samuels, W. D. and Exarhos, G. J., Synthesis of SiC nanorods from bleached wood pulp. *Mater. Lett.*, 2007, **61**, 2814–2817.